[Surface Science **602** (2008) 2039-2046]

Core Level Spectroscopy of the Ni/W(110) Interface: Correlation of W Interfacial Core Level Shifts with First-Layer Ni Phases

D. M. Riffe [a,*], R. T. Franckowiak [a], N. D. Shinn [b], B. Kim [c,d], K. J. Kim [e], and T.-H Kang [d]

[a] *Physics Department, Utah State University, Logan, UT 84322-4415*
[b] *Sandia National Laboratories, Albuquerque, NM, 87185, USA*
[c] *Department of Physics, POSTECH, Pohang, Kyungbuk 790-784, Korea*
[d] *Beamline Research Division, Pohang Accelerator Laboratory (PAL), Pohang, Kyungbuk 790-784, Korea*
[e] *Department of Physics, Konkuk University, Seoul 143-701, Korea*

(Dated: April 16, 2008)

Abstract
We have measured W $4f_{7/2}$ core-level photoemission spectra from W(110) in the presence of Ni overlayers, from ∼0.2 to ∼3 monolayers. Interfacial core-level shifts associated with first-layer Ni phases have been identified: -230 ± 15 meV for the 1×1 pseudomorphic phase and -70 ± 7 meV for the 7×1 close-packed commensurate phase. At higher Ni coverages the interfacial core-level shift is -100 ± 10 meV. These shifts are analyzed using the partial-shift model of Nilsson *et al.* [Phys. Rev. B 38 (1988) 10357]; the analysis indicates that the difference in binding energies between the 1×1 and 7×1 phases has a large contribution from structural differences between the two phases.

Keywords: Bimetallic surfaces; Nickel; Soft X-ray photoelectron spectroscopy; Surface electronic structure; Tungsten

*Corresponding author. Tel.: +1 435 797 3896; ax: +1 435 797 2491. *E-mail address*: riffe@cc.usu.edu (D. M. Riffe).

1. Introduction

Due to the unique chemical, optical, and magnetic properties of nanostructured materials, bimetallic epitaxial systems have received considerable scientific attention. In particular, the interface formed by ultrathin Ni layers grown on W(110) has been extensively studied as a model bimetallic system [1-35], in part because it is an excellent system for relating electronic structure to morphology. Using various surface analysis techniques, including low energy electron diffraction (LEED), Auger electron spectroscopy (AES), thermal desorption spectroscopy (TDS), work-function measurements, reflection high energy electron diffraction (RHEED), and/or high-energy ion scattering (HEIS), a number of early studies investigated the structure and morphology of the Ni layers as a function of Ni coverage [1-7]. Other early investigations probed the electronic structure of the Ni/W(110) interface using valence-band angle-resolved photoelectron spectroscopy (ARPES) and core-level x-ray photoelectron spectroscopy (XPS) [8-12]. Taken together, these early studies indicate that the first-layer Ni film is initially pseudomorphic (ps), followed by sequential transitions to two commensurate phases – an 8×1 phase followed by a 7×1 close-packed (cp) phase. Further adsorption results in quasi-van-der-Merwe growth up to ∼3 Ni overlayers [at room temperature (RT)]. More recently, scanning tunneling microscopy (STM) has been utilized to investigate this interface; the STM measurements confirm the results of the earlier structural work and also demonstrate the coexistence of the ps and cp phases [18-20]. Scanning tunneling microscopy has also been combined with measurements of changes in surface stress in order to investigate the relationship between the structure of the first layer and stress at the interface [17, 18]. Very recently, the structure of the 7×1 cp phase has been probed with x-ray diffraction; the results suggest a major reconstruction of the W surface atoms for this phase [21]. In addition to these basic structural and electronic studies of Ni/W(110), the chemical and catalytic properties of this interface have been extensively investigated [4, 11, 22-27]. There have also been numerous measurements of the magnetic properties of Ni/W(110) thin films [28-33], which have been extended to epitaxial Fe films grown on Ni/W(110) [36-41]. Femtosecond electron dynamics in Ni/W(110) films have also been investigated [34, 35].

Here we use XPS of the W $4f_{7/2}$ core level to follow the growth of Ni films on W(110) from ∼0.2 to ∼3.5 ps monolayers (ML's) [42]. The combination of the sharpness of the W $4f_{7/2}$ core level and the simple core-level structure of W(110) make this face of W an ideal substrate for XPS investigation of interfacial electronic structure. This has been previously taken advantage of in investigations of hydrogen [43, 44], oxygen [45-48], metallic overlayers [12, 49-58], and mixtures of metallic overlayers and oxygen on W(110) [47, 49, 59-62].

The goal of the present investigation is to see how electronic structure, as reflected in core-level shifts, is connected to the Ni structures that have been previously observed. From our measurements we identify W interfacial core-level shifts associated with the 1×1 ps and 7×1 cp phases of the first Ni layer. Somewhat surprisingly, only a single core-level feature is associated

with the 7×1 phase, even though the commensurate nature of this phase means that not all surface W atoms have the same Ni-atom coordination. Furthermore, we observe a relatively large shift in the W core-level binding energy between the 1×1 and 7×1 phases. This large difference indicates that structural differences (rather than simply Ni-coverage differences) between the 1×1 and 7×1 phases are responsible for much of the difference in W $4f$ binding energies associated with these two phases. In order to gain insight into how structure may contribute to core-level binding-energy differences, we employ the partial-shift model of Nilsson and coworkers [63] to analyze the interfacial core-level shifts. With reasonable values of the input parameters, we find that the partial-shift model is able to reproduce the experimental core-level binding energies associated with the Ni/W(110) interface.

2. Experimental details

The W $4f_{7/2}$ spectra were obtained using beamline U16A at the National Synchrotron Light Source. The beamline includes a 6-m torodial-grating-monochromator and an end station with a 150 mm radius hemispherical electron-energy analyzer. An incident photon energy of 72 eV was used to maximize the signal from the first W layer. The total resolution (monochromator and analyzer) was ∼140 meV.

The W surface was cleaned by the standard technique of annealing the sample at 1550 K in an oxygen environment with periodic flashes to 2400 K [64]. As discussed in detail below, cleanliness is assessed via the W $4f_{7/2}$ photoemission spectra. From our assessment we estimate surface contamination to be <1% of a ps ML.

Nickel layers were deposited on the W surface at room temperature from a shuttered, electron-beam evaporator that is surrounded by a liquid-nitrogen-cooled shroud. Most of the Ni overlayers were grown at a rate of ∼0.34 ps ML/min, although layers grown at other rates do not appear to be substantially different from those grown at this rate.

3. Results and analysis

The data in Fig. 1 illustrate the evolution of the W(110) $4f_{7/2}$ spectrum upon increasing Ni coverage. The clean-surface spectrum consists of two peaks: the lower binding-energy (BE) peak (surface) is from W atoms in the first atomic layer, and the higher BE peak (bulk) is from W atoms in the second atomic layer and deeper [65, 66]. The solid and dashed lines in Fig. 1 mark the BE's of the bulk and clean-surface atoms, respectively. As is evident in Fig. 1, with increasing Ni exposure the surface peak diminishes in size until only one peak is visible. Notice that this single peak is at a slightly lower BE than the bulk peak of the clean surface, indicating that the core levels of the Ni influenced atoms have a BE that is close to, but slightly lower than, the bulk atoms. Other core-level studies of the growth of transition metal layers on W surfaces have shown that, in general, a transition-metal overlayer increases the core-level BEs of the first-layer tungsten atoms [12, 49, 54, 55, 58, 67-72]. Our data clearly exhibit this same behavior.

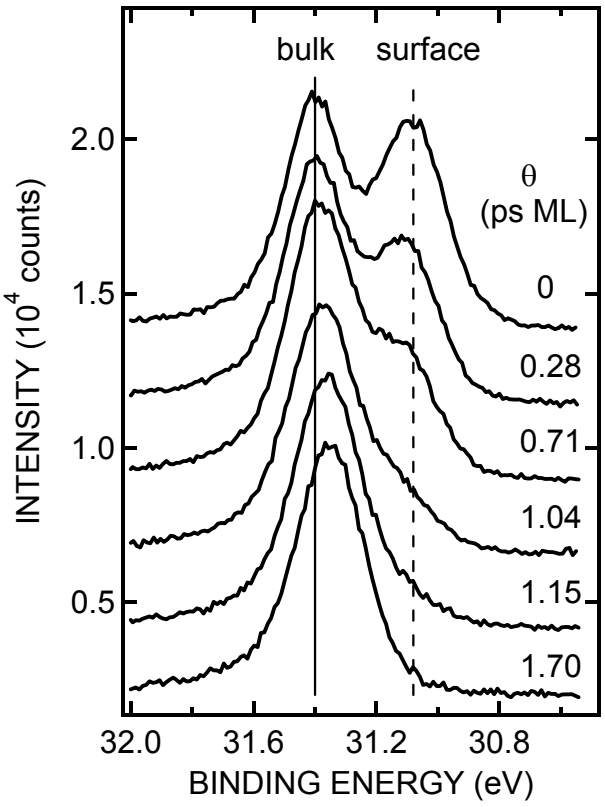

FIG. 1 W4f$_{7/2}$ core level spectra from the Ni/W(110) bimetallic interface, illustrating the effect of increasing Ni coverage. The solid and dashed lines mark the positions of the bulk and clean-surface core-level features, respectively.

We use least-squares fitting to decompose the core-level data into spectral components. It has been previously shown [66] that each W $4f$ core-level photoemission feature is well described by a Gaussian broadened Doniach-Šunjic (DS) peak [73], which is described by five parameters: a lifetime width, singularity index, binding energy, peak height, and Gaussian width. The Gaussian width has phonon, instrumental, and (possibly) inhomogeneous contributions. We use a linear function to describe the background.

Figure 2(a) illustrates a least-squares fit to a clean-surface spectrum. The fit is dominated by two components, one marked S (surface) and one marked B (bulk). However, in order to get a satisfactory least-squares fit to spectra from the clean surface it is necessary to add in a third, much smaller component at higher binding energy (275 ± 30 meV), which we label I_3. Based on a comparison of shifts induced by C on W(100) [74], we suspect that this peak is due to residual C on the surface. Given the size of this peak (2.5 ± 0.2 % of the surface $4f_{7/2}$

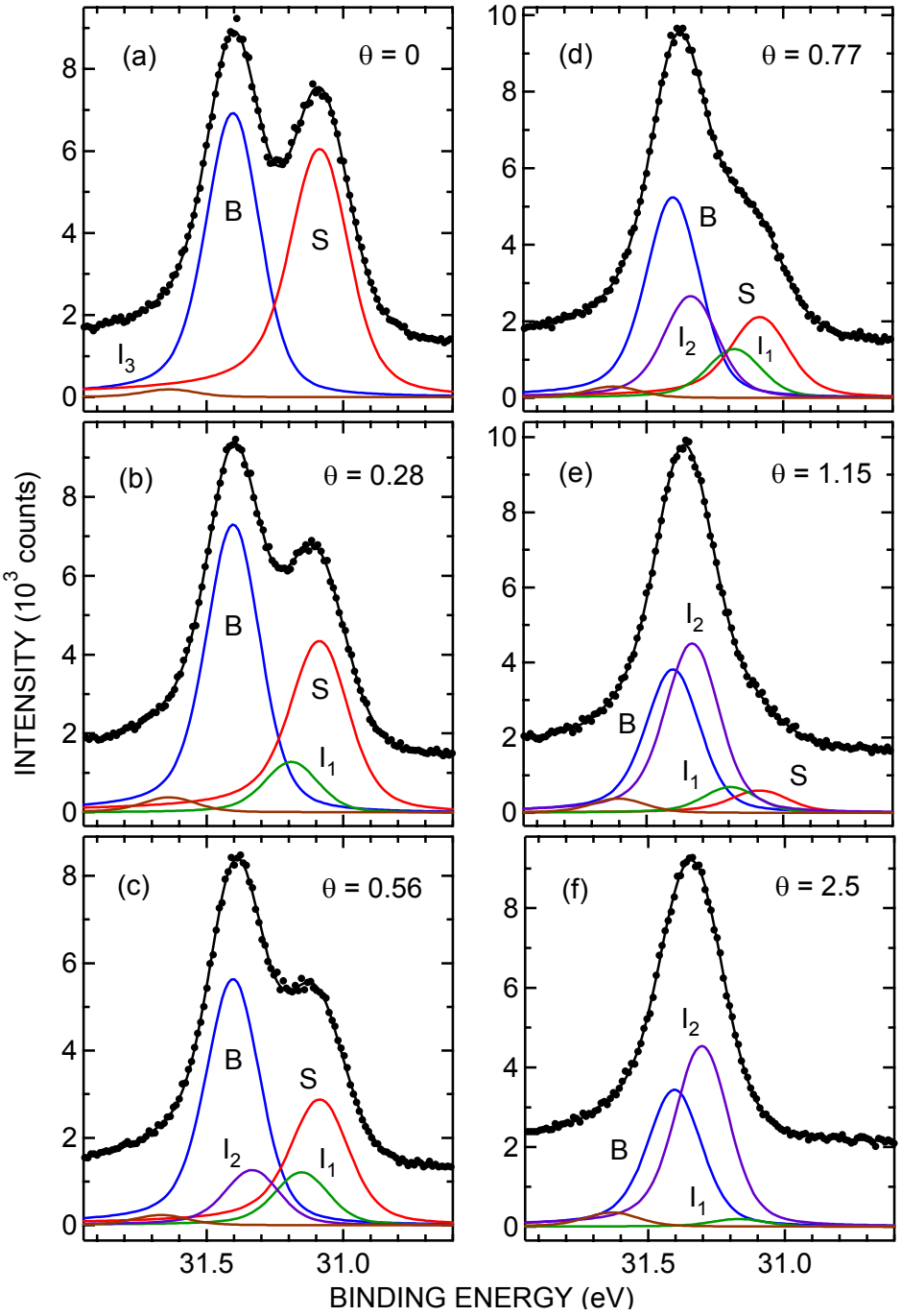

FIG. 2 Least-squares analysis of W $4f_{7/2}$ core level spectra from the Ni/W(110) bimetallic interface. Peaks due to bulk W (B), clean-surface W (S), and W atoms covered by 1×1 ps Ni (I_1) and 8×1 and 7×1 cp Ni (I_2) are shown. A third, much smaller interface peak [I_3 in (a)] is also shown. Indicated coverages of Ni are in units of a ps ML.

spectrum) and the expectation that C sits in the quasi-three-fold hollow site, we estimate the contamination to be <1% of a ps ML.

Because the Ni-induced components of the spectra are not resolved, we find it necessary to constrain certain parameters in fitting the Ni/W(110) spectra. First, the lifetime widths and singularity indices of the B and S features are held to values obtained from data obtained at significantly higher resolution [66]. Second, because the B and S components have nearly identical phonon broadenings [66], the Gaussian widths of the B and S features are constrained to the same (fitted) value. Third, the BE difference between the B and S components [which is known as the surface core-level shift (SCS)] is main-

tained at its clean-surface value [66]. Lastly, because the first-layer W atoms become more highly coordinated in the presence of the Ni-overlayer atoms, we assume that the lifetime width, singularity index, and Gaussian width of the Ni-induced components are the same as the B feature. This last assumption is not critical, however: least-squares analyses in which the Ni-induced features are assumed to have the same line shape as the S peak, for example, do not produce substantially different results.

With these constraints the least-squares analysis provides the following insights into the spectra from the Ni covered surface. As shown in Fig. 2(b) – 2(f), Ni adsorption produces two other core-level features, labeled I_1 and I_2, which, as discussed in more detail below, are due to first-layer W atoms that are bonded to first-overlayer Ni atoms. The component labeled I_1 appears with the initial growth of the Ni layer and has an interfacial core-level shift (ICS) of -230 ± 15 meV [75]. Within the precision of the measurement, this shift is independent of Ni coverage. The component labeled I_2 has a delayed appearance and an ICS of -70 ± 7 meV at coverages between 0.65 and 1.3 ps ML (see details of the coverage determinations below). Due to its small size at Ni coverages below 0.65 ps ML, the BE of this peak cannot be reliably determined, so in analyses of those spectra the shift of this peak was held fixed at -70 meV. For higher Ni coverages the BE of the I_2 peak decreases, resulting in an ICS of -100 ± 10 meV.

In fitting all of the spectra we also must include the I_3 component [only labeled in Fig. 2(a)] at higher BE. Its BE and intensity systematically vary with Ni coverage. However, given its small intensity at all Ni coverages, it is not believed to be associated with surface W atoms covered by a particular phase of Ni, but is likely from W atoms coordinated by both C and Ni atoms.

4. Discussion

4.1. Assignments of spectral components and determination of Ni coverages

In this section we assign the I_1 and I_2 components to Ni phases and use the core-level intensities to determine the Ni coverages associated with each spectrum. As will be evident, these two processes are not sequential, but are intertwined. We begin by reviewing the details of results from structural studies of W(110); these results enable us to immediately assign the I_1 component to the 1×1 ps phase. Given this assignment, we then use the relative intensities of the S, I_1, and I_2 components to ascertain that the I_2 phase is associated with both the 8×1 and 7×1 commensurate phases. With these structural assignments to the I_1 and I_2 features, we then determine the Ni coverage for each core-level spectrum at coverages less than ∼1.3 ps ML (∼1 cp ML). These absolute coverages then allow us to infer the Ni adsorption rate (for a given evaporator setting), which, in turn, enables us to infer Ni coverages greater than ∼1.3 ps ML.

The structure of the first Ni layer has been previously delineated in a number of studies. Initially, the first overlayer grows in 1×1 pseudomorphic (ps) islands [1, 7]. Although the ps phase is believed to be thermodynamically stable up to a full ML [7, 14], limited diffusion at RT induces a transition to the 8×1 commensurate phase at a lower coverage. Depending upon the amount of residual gas contamination and/or the density of steps [7], this transition begins somewhere between ∼0.25 and ∼0.9 ps ML [1, 10, 18-20, 40]. The density of the 8×1 phase is not universally agreed upon [20]: some researchers favor a density of 1.59×10^{15} atoms cm^2 (which occurs if there are 9 Ni-atom spacings per 8 W-atom spacings along the [001] direction) [18, 19], while others favor a more closely packed density of 1.77×10^{15} atoms cm^2, (which occurs if there are 10 Ni-atom spacings per 8 W-atom spacings) [1]. With increasing Ni coverage the 8×1 phase transforms into the 7×1 cp phase at a coverage between ∼0.5 and ∼1.28 ps ML [18-21]. The local coverage of the 7×1 phase is taken to be 1.82×10^{15} atoms cm^2, which arises from having 9 Ni-atoms spacings per 7 W-atoms spacing along [001]. A full 7×1 layer corresponds to 1.28 ps ML of adsorbed Ni [18-21].

Using this structural information, we can begin to assign the Ni-induced core-level features to particular phases of the first Ni overlayer. Given that only the I_1 peak appears at the lowest Ni coverages, we assign this peak to W atoms that are covered by ps regions of the first Ni layer. Similarly, because the I_2 peak does not appear until significant Ni adsorption occurs, it must be associated with the 8×1 and/or the 7×1 phases. However, before more precise identification of the I_2 feature can take place we must first establish the Ni coverage at which this feature appears.

We use the relative intensities of the I_1, I_2, and S peaks to estimate the absolute Ni coverage associated with a given spectrum. Assuming that the ith core-level peak is associated with a particular local coverage θ_i, the total Ni coverage θ can be simply written as the weighted average over all local coverages

$$\theta = \frac{\sum_i \theta_i \, F_i \, e^{d_i/\lambda}}{\sum_i F_i \, e^{d_i/\lambda}}, \qquad (1)$$

where the weight function $F_i \, e^{d_i/\lambda}$ is the product of the integrated intensity F_i of a particular core-level line and a factor $e^{d_i/\lambda}$ that accounts for the attenuation of the intensity due to the Ni overlayer. In this second factor d_i is the thickness of the ith overlayer, and λ is the inelastic mean free path in Ni. We estimate the overlayer thickness from the ratio of the surface density (for a given layer) to the volume density of Ni. For λ we use a value of 6 Å [76]. The sums in Eq. (1) are over all spectral features associated with the first layer of W atoms. For the clean-surface atoms $\theta_i = 0$ and for the ps-layer-covered atoms $\theta_i = 1$ (neglecting island-edge effects). Equation (1) is also predicated on insignificant variations in component intensities due to electron diffraction. We point out that

we have previously used an equation similar to Eq. (1) to determine the coverage of O on W(110) [47].

Applying Eq. (1) to our spectrum with the largest I_1 component, but no I_2 component, yields a coverage of 0.3 ps ML. At coverages slightly above this we begin to also observe the I_2 component. Given that the lowest observed coverages for the 8×1 and 7×1 phases are 0.25 and 0.5 ps ML, respectively, we can thus associate the initial appearance of the I_2 component with the 8×1 phase. However, because the I_2 component persists at substantially larger Ni exposures, this component must also be associated with the 7×1 phase at higher coverages.

In order to determine the coverages between 0.3 and ∼1.3 ps ML (∼1 cp ML), we need to know the local coverages of the 8×1 and 7×1 Ni phases. As discussed above, for the 7×1 phase $\theta_i = 1.28$. For the 8×1 phase $\theta_i = 1.12$ or $\theta_i = 1.25$, depending upon the correct structure. Because we observe no significant change in BE of the I_2 component (at sub-cp-ML coverages), we favor the higher-density model for the 8×1 phase. Given this and the fact that 1.28 and 1.25 are negligibly different, we simply use $\theta_i = 1.28$ for the I_2 peak for all coverages. (We note that if we use $\theta_i = 1.12$ at the lower Ni coverages, the calculated coverage changes by <10 %, and so this choice is not critical.) Using this procedure we have determined the first-layer Ni coverage associated with each spectrum at a coverage <∼1.3 ps ML.

As a check on this procedure, we compare the coverage calculated via Eq. (1) with the Ni-exposure time for a set of spectra obtained at identical evaporator settings. This comparison, shown in Fig. 3, exhibits the expected linear relationship. From the slope of a linear fit to the data, shown as the solid line in the figure, we determine a growth rate of 0.34 ± 0.04 ps ML/min. Satisfyingly, the intercept of the fit passes very close to the origin.

Using this growth rate we have estimated the Ni coverage for spectra from Ni layers with coverages >∼1.3 ps ML, such as that shown in Fig. 2(f). We note that because these coverage values are not directly inferred from each individual spectrum, they are less precise than the values at lower Ni coverages.

Our results are summarized in both Fig. (4) and Table I. In Fig. (4) we present the fractional intensities of the S, I_1 and I_2 peaks and the ICS's vs Ni coverage. As is evident in part (b) of the figure, the <1.5 ps ML shifts of the I_1 and I_2 components are independent of Ni coverage. Above 1.5 ps ML the I_2 BE also appears to be constant, but at a slightly lower BE. Table I summarizes the results for the shifts: in the table we list the (clean surface) SCS and Ni-induced ICS's. We also list the shift of each peak with respect to the clean-surface BE; this shift is known as the adhesion core-level shift (ACS) [77]. Note that the ACS is equal to the ICS minus the SCS.

4.2 Core-level spectra and interfacial structure

Perhaps the biggest surprise to emerge from our analysis is the result that only one W core-level peak is observed for the commensurate 7×1 phase, even though not all of the first layer W atoms have the same Ni-atom coordination in this phase. (For example, the structural model proposed to explain x-ray diffraction from the 7×1 phase has 4 inequivalent W atoms in the first layer [21].) At a minimum such inequivalence might be expected to inhomogeneously broaden the associated core-level peak, but our analysis indicates that such broadening is not necessary. This is in dramatic contrast to W core-level results from O/W(110), which show that the W core-level binding energy is sensitive not only to the O-atom coordination number but also the exact location of the coordinating O atoms [47]. Given that the O-W bond is best described as polarized-covalent while the Ni-W bond is best described as metallic, we suggest that the uniform core-level binding energy for a given phase of Ni is due to the metallic nature of the bonding between the W and Ni layers.

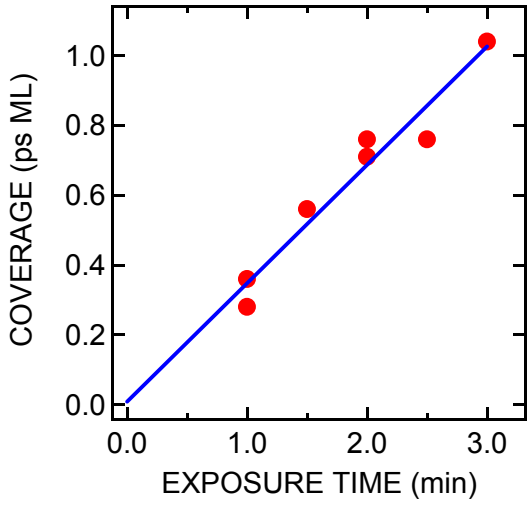

FIG. 3 Ni coverages deduce from Eq. (1) as a function of Ni exposure time. The solid line is a linear fit to the data, indicating a growth rate of ∼0.34 ps ML/min.

Another unanticipated result from our measurements is the rather large difference in the core-level BE's associated with the 1×1 ps and 7×1 cp phases. Intuitively we expect the shift with respect to the clean-surface BE (the ACS) to be proportional to the local overlayer coverage. Simple theory supports this notion (see below). However, this is clearly not observed for Ni/W(110): for the 7×1 and 1×1 phases the ratio of the ACS's is 2.8 ± 0.5, which is much greater than the coverage ratio of 1.28. This discrepancy indicates that structural differences between the two layers likely contribute to the core-level shifts. This is discussed in detail in Sec. 4.3.

Coexistence of the 1×1 and commensurate phases is evident in Fig 4(a), which shows that some 1×1 phase persists even in the presence of up to ∼3.5 ps ML of Ni (which corresponds to ∼2.7 overlayers). Our data on this coexistence can be compared with the STM data of

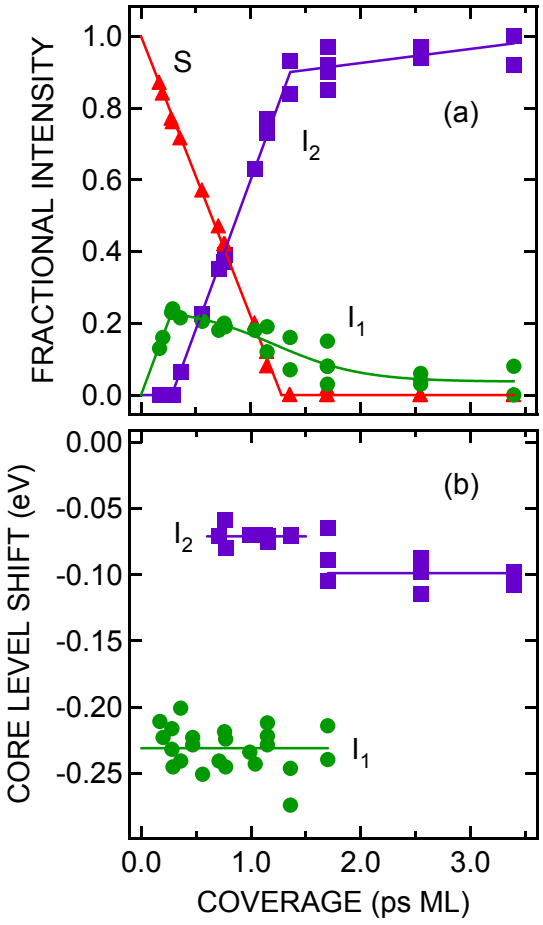

FIG. 4 Fractional intensity (a) and interfacial core-level shifts (ICS's) (b) as a function of Ni coverage. The intensities are the fraction of the total surface intensity. The solid lines are guides to the eye.

Sander and coworkers [18, 19]. For a coverage of ∼1.2 ps ML Sander *et al.* observe an interface in which the 7×1 phases covers about 90% of the surface. The remainder of the surface is covered by the 1×1 phase and bare patches that expose the underlying W surface. From Figure 4 we can estimate that we have 80% 7×1, 14% 1×1, and 6% bare patches at this same coverage, in reasonable agreement with the STM observations.

Figure 4 also shows that the second Ni layer influences the BE of the of the I_2 peak, causing it to shift from −70 meV to −100 meV. Interestingly, we do not observe a gradual transition in the BE of the I_2 component. A given spectrum exhibits either a shift close to −70 meV or a shift close to −100 meV. It is further noteworthy that the transition occurs for a Ni coverage that is only slightly in excess of 1 atomic layer (1 cp ML = 1.28 ps ML). However, as noted above, due to the nature of the coverage determination above 1 cp ML, we cannot ascertain a precise value of the coverage where this transition occurs.

4.3 Born-Haber cycle analysis of the Ni-induced shifts

A core-electron BE is the difference in energy between the initial (ground) state of the system and a final (excited) state that consists of a core hole located on a particular atom. In a metallic system the BE is associated with a final state that is optimally screened by the valence charge. A core-level shift is thus the energy difference of two different final states with a core hole located on two inequivalent, fully screened atoms.

There have been a number of approaches, using Born-Haber cycles, to describe these energy differences [63, 77-81]. The approach most useful for discussing shifts at a bimetallic interface is the partial-shift model of Nilsson *et al.* [63], which we utilize to discuss the Ni induced shifts measured here. In the partial-shift model the core-level binding energy of a Z atom (W, in the present case) in environment E can be written as

$$\begin{array}{c} \varepsilon_c^{(E)}(Z) = \varepsilon_c^0(Z) + c_Z^{(E)} E_{sol}^{Z^*}(Z) \\ +c_M^{(E)}\left[E_{sol}^{Z^*}(M) - E_{sol}^{Z}(M)\right] \\ +c_V^{(E)}\left[E_{coh}^{Z^*} - E_{coh}^{Z}\right] \end{array} , \qquad (2)$$

where, for example, $E_{sol}^{Z}(M)$ is the solution energy of a Z atom in an M metal (Ni, in the present case) host, and E_{coh}^{Z} is the cohesive energy of the Z metal. A core-excited (and fully screened) Z atom is designated by Z^*. The parameter ε_c^0 is a reference binding energy, the value of which is unimportant because Eq. (2) is only used to calculate differences in $\varepsilon_c^{(E)}(Z)$ for Z atoms in two different environments. The parameters $c_Z^{(E)}$, $c_M^{(E)}$, and $c_V^{(E)}$ are effective concentrations of neighboring Z atoms, M atoms, and the vacuum, respectively, surrounding the Z atom in the environment E. Often the simplifying assumption $c_Z^{(E)} + c_M^{(E)} + c_V^{(E)} = 1$ is used, although this is not an absolute constraint [63, 82]. For a bulk Z atom $c_M^{(B)} = 0$, $c_V^{(B)} = 0$, and $c_Z^{(B)} = 1$ (by definition). For a W(110) surface atom $c_M^{(S)} = 0$ (by definition), and we expect $c_Z^{(S)} \approx 0.8$ and $c_V^{(S)} \approx 0.2$. These two expectations come from the observation that for closed packed surfaces the surface energy (per atom) is approximately 20% of the cohesive energy [83, 84]. For a W atom at the Ni/W interface, we expect $c_Z^{(I)}$ close to $c_Z^{(S)}$, $c_M^{(I)}$ close to $c_V^{(S)}$, and $c_V^{(I)}$ close to zero, with the exact values dependent upon the structure of the interface.

Because the ACS is a somewhat more intuitive quantity that the ICS, we concentrate on the ACS in the following discussion. Using Eq. (2) we can express the adhesion core-level shift $\Delta\varepsilon_c^{(I,S)}(Z)$ as

$$\begin{array}{c} \Delta\varepsilon_c^{(I,S)}(Z) = \left[c_Z^{(I)} - c_Z^{(S)}\right] E_{sol}^{Z^*}(Z) \\ +c_M^{(I)}\left[E_{sol}^{Z^*}(M) - E_{sol}^{Z}(M)\right] \\ +\left[c_V^{(I)} - c_V^{(S)}\right]\left[E_{coh}^{Z^*} - E_{coh}^{Z}\right] \end{array} , \qquad (3)$$

TABLE I Ni-layer induced W core-level shifts at low-index W surfaces.

Surface	SCS (meV)	Ni layer(s)	ICS (meV)	ACS (meV)
W(110) [a]	−320	1×1 ps	-230 ± 15	90 ± 15
		7×1 cp	-70 ± 7	250 ± 7
		> ∼1.5 ps ML	-100 ± 10	220 ± 10
W(110) [b]		∼1 ML	-140 ± 20	180 ± 20
W(111) [c]	−337	1 physical ML	−210	127
W(100) [d]	−360	1×1 ps	−120	240
		> 2 ps ML	−170	190

[a]This study.

[b]N. D. Shinn, B. Kim, A. B. Andrews, J. L Erskine, K. J. Kim, and T.-H Kang, Mat. Res. Soc. Symp. Proc. 307 (1993) 167.

[c]H.-S Tao, J. E. Rowe, T. E. Madey, Surf. Sci. 407 (1998) L640. The SCS, ICS, and AS values for W(111) are average values for the first three surface layers. See text for more detail.

[d]S. H. Overbury, P. F. Flynn, D. R. Mullins, N. D. Shinn, Surf. Sci. 339 (1995) 68.

where we have used the fact that $c_M^{(S)} = 0$. If we assume that the Ni layer does not change the effective concentration of Z atoms surrounding the first-layer W atoms (so that $c_Z^{(I)} = c_Z^{(S)}$), and we also use the constraint $c_Z^{(E)} + c_M^{(E)} + c_V^{(E)} = 1$, then Eq. (4) simplifies to

$$\Delta\varepsilon_c^{(I,S)}(Z) = c_M^{(I)} \left[E_{sol}^{Z^*}(M) - E_{sol}^{Z}(M) - \left(E_{coh}^{Z^*} - E_{coh}^{Z} \right) \right]. \quad (4)$$

Equation (5) exhibits the intuitive expectation that the adlayer-induced shift of the surface-peak BE should be proportional to the concentration of M atoms in the overlayer [as long as the energy terms in Eq. (5) are constant]. However, as discussed above, this expectation is not met in the comparison of the 1×1 and 7×1 phases.

This lack of agreement implies that if the Ni-induced shifts are to be described by the partial-shift model, we must consider variations in additional model parameters. There are two physically reasonable candidates for such variations. The first is $\left[E_{sol}^{Z^*}(M) - E_{sol}^{Z}(M) \right]$, which may vary due to structural differences in the two Ni adlayers [85, 86]. The second candidate is $c_Z^{(I)}$, which may differ due to reconstruction of the first W layer [21].

In order to ascertain how the ACS's might be affected by such variations, we need values for the various cohesive and solution energies, some of which involve the core-excited (Z^*) atom. For these Z^* terms we utilize the oft-made approximation that a Z^* atom is chemically equivalent to a $Z+1$ atom (Re, in the present case) [78]. In this so-called equivalent-cores approximation Z^* is replaced by $Z+1$ in expressions such as Eqs. (2) - (5). For W atoms with a $4f$ core hole this approximation has been investigated in some detail. Because of the non-zero spatial extent of the $4f$ level, the equivalent-cores approximation is only very approximate. *Ab initio* calculations have shown that the equivalent cores approximation gives a SCS for W(110) that is smaller in magnitude than the experimental or Z^*-calculated shift by 0.1 eV [87]. Thus, in utilizing the equivalent-cores approximation, we scale all calculated shifts by 0.32/0.22, the ratio of the actual SCS to the equivalent-cores calculated shift.

We first consider the possibility that $\left[E_{sol}^{\mathrm{Re}}(\mathrm{Ni}) - E_{sol}^{\mathrm{W}}(\mathrm{Ni}) \right]$ may be different for the 7×1 and 1×1 phases. That this might be so is supported by recent *ab initio* calculations of the structural contribution to solution energies of $4d$ transition-metal atoms in $4d$ transition metal hosts [86]. The calculations (for the $4d$ atoms that are isoelectronic to the atoms of interest here) show that $\left[E_{sol}^{\mathrm{Tc}}(\mathrm{Pd}) - E_{sol}^{\mathrm{Mo}}(\mathrm{Pd}) \right]$ for bcc Pd is ∼0.4 eV lower than $\left[E_{sol}^{\mathrm{Tc}}(\mathrm{Pd}) - E_{sol}^{\mathrm{Mo}}(\mathrm{Pd}) \right]$ for hcp Pd. Because the 1×1 ps Ni layer has the structure of the underlying bcc lattice, while the 7×1 cp layer is consistent with the Ni atoms in a slightly distorted fcc (or hcp) closed-packed arrangement [1, 10], we expect a similar difference in $\left[E_{sol}^{\mathrm{Re}}(\mathrm{Ni}) - E_{sol}^{\mathrm{W}}(\mathrm{Ni}) \right]$ for these two layers, which could help explain the difference in ACS's.

A more quantitative assessment of this possibility requires values for $\left[E_{coh}^{\mathrm{Re}} - E_{coh}^{\mathrm{W}} \right]$ and $\left[E_{sol}^{\mathrm{Re}}(\mathrm{Ni}) - E_{sol}^{\mathrm{W}}(\mathrm{Ni}) \right]$. For $\left[E_{coh}^{\mathrm{Re}} - E_{coh}^{\mathrm{W}} \right]$ we use experimental values of the cohesive energies, $E_{coh}^{\mathrm{Re}} = 8.031$ eV and $E_{coh}^{\mathrm{W}} = 8.899$ eV [88, p. 50]. We point out that $c_V^{(S)} \left[E_{coh}^{\mathrm{Re}} - E_{coh}^{\mathrm{W}} \right]$ can be interpreted as the difference in surface energies of Re and W, which for $c_V^{(S)} = 0.2$ gives −0.174 eV, a value that is quite close to the surface-energy difference of −0.18 eV calculated by Ruban *et al.* [84]. For $\left[E_{sol}^{Re}(\mathrm{Ni}) - E_{sol}^{\mathrm{W}}(\mathrm{Ni}) \right]$ the semiempirical theory of Miedema gives $\left[E_{sol}^{\mathrm{Re}}(\mathrm{Ni}) - E_{sol}^{\mathrm{W}}(\mathrm{Ni}) \right] = 0.00$ eV [85], which applies to fcc Ni. Using $\left[E_{coh}^{\mathrm{Re}} - E_{coh}^{\mathrm{W}} \right] = -0.87$ eV, $\left[E_{sol}^{\mathrm{Re}}(\mathrm{Ni}) - E_{sol}^{\mathrm{W}}(\mathrm{Ni}) \right] = 0.00$ eV, and our experimental result of 0.25 eV for the 7×1 ACS in Eq. (5) implies that $c_M^{(7\times1)} = 0.20$. This result is entirely

sensible: for a close-packed Ni layer on top of W(110) we would expect the Ni-atom concentration $c_M^{(I)}$ to have fully replaced the vacuum concentration $c_V^{(S)}$. If we further assume that $c_M^{(1\times1)} = 0.15$ (so that $c_M^{(7\times1)} \Big/ c_M^{(1\times1)}$ is essentially the ratio of Ni-atom coverages), then Eq. (5) further implies that $\left[E_{sol}^{\rm Re}({\rm Ni}) - E_{sol}^{\rm W}({\rm Ni})\right] = -0.45$ eV for the 1×1 phase. Given the *ab initio* calculated difference in $\left[E_{sol}^{\rm Tc}({\rm Pd}) - E_{sol}^{\rm Mo}({\rm Pd})\right]$ for hcp and bcc Pd, this result for $\left[E_{sol}^{Re}({\rm Ni}) - E_{sol}^{\rm W}({\rm Ni})\right]$ also appears to be entirely reasonable.

Of course, there may be another structural contribution to the measured shifts. Results from a recent x-ray diffraction study has lead to the interpretation of significant reconstruction of the first-layer W atoms [21]. Thus, we might expect some differences in $c_Z^{(E)}$ among the clean, 1×1, and 7×1 surfaces. In order to assess the effect of variations in $c_Z^{(E)}$ we need a value for $E_{sol}^{\rm Re}({\rm W})$, which we can estimate from the partial-shift expression for the SCS

$$\Delta\varepsilon_c^{(S,B)}(Z) = \left[c_Z^{(S)} - 1\right] E_{sol}^{Z*}(Z) + c_V^{(S)} \left[E_{coh}^{Z*} - E_{coh}^{Z}\right]. \quad (5)$$

Applying this equation to the experimental SCS of W(110) in the equivalent-cores approximation (with $c_Z^{(S)} = 0.8$ and $c_V^{(S)} = 0.2$) yields $E_{sol}^{Re}({\rm W}) = 0.23$ eV. This is somewhat larger than Miedema's semiempirical value of −0.03 eV [85]. However, there is evidence that 0.23 eV is a more accurate value for $E_{sol}^{Re}({\rm W})$: a recent calculation of the isoelectronic term with 4*d* metals yields $E_{sol}^{\rm Tc}({\rm Mo}) = 0.28$ eV [86]. We thus use the value of 0.23 eV for $E_{sol}^{Re}({\rm W})$.

Using Eq. (4) we find that we can also reproduce the measured ACS's with the following parameters: $c_Z^{(1\times1)} = 0.75$, $c_M^{(1\times1)} = 0.15$, $c_V^{(1\times1)} = 0.1$, $c_Z^{(7\times1)} = 0.85$, $c_M^{(7\times1)} = 0.20$, $c_V^{(7\times1)} = 0.0$, and $\left[E_{sol}^{\rm Re}({\rm Ni}) - E_{sol}^{\rm W}({\rm Ni})\right] = -0.09$ eV (for both phases). These parameters may also be entirely reasonable, although it is not clear *a priori* how the proposed reconstruction should affect $c_Z^{(E)}$. *Ab initio* calculations of the W core-level shifts in the presence of a 7×1 Ni layer (both with and without the inferred W reconstruction [21]) would help to identify the exact nature of the induced shifts.

The change in 4*f* binding energy above ∼1.5 ps ML is also likely due to a structural effect. We suggest that a slight amount of second-layer Ni induces a slight structural rearrangement in the first-layer Ni and/or the surface W atoms. The small −0.030 eV shift (compared to the 7×1 phase) can be explained by a either a change in $\left[E_{sol}^{Re}({\rm Ni}) - E_{sol}^{\rm W}({\rm Ni})\right]$ of −0.11 eV or a change in $c_Z^{(7\times1)}$ of −0.05.

4.4 Comparisons with other Ni/W core level data

Core-level shifts induced by Ni layers on W(111), W(100), and W(110) have been previously measured. Along with the results from our present study, the results from these prior studies are summarized in Table 1.

Previously Shinn and coworkers measured an ICS of −140±20 meV on W(110), which they assigned to ∼1ML of Ni. This shift does not agree very well with any shift determined in the present study, but it is closest to our ICS of −100 ± 10 meV for coverage greater than ∼1.5 ps ML. In that earlier study Shinn *et al.* presented two Ni/W(110) spectra, which they associated with ∼0.5 and ∼1 ML of Ni. However, a comparison of their ∼0.5 ML spectrum {Fig. 2(b) in [12]} with our spectra [Fig. (2)] suggests that their ∼0.5 ML spectrum is from a surface with a coverage that is closer to 0.8 ps ML. We thus propose that their ∼1 ML spectrum is actually from W(110) covered by a sufficient amount of second-layer Ni to induce the −70 meV to −100 meV ICS transition that we observe in this study. With this interpretation of the previous data, the results of the two W(110) studies are in reasonable agreement with each other.

Core-level spectra from Ni-covered W(111) have been obtained by Tao and coworkers [69]. The W(111) surface is rather open, enabling atoms in the first three layers to directly bond with the Ni-layer atoms. This openness leads, for the clean surface, to core-level binding energies for the first three layers that are distinct from the bulk [89, 90]: SCS's obtained from the high-resolution spectra of Tao *et al.* are −446, −446, and −121 meV for atoms in the first, second, and third layers, respectively [69]. In Table 1 we list the average SCS of −337 meV for this surface. The core-level measurements of Tao *et al.* were obtained for ∼1 physical ML of Ni, where a physical ML is a pseudomorphic overlayer in which each W atom in the first three layers is covered by a Ni atom. The core-level BE's in the first three W surface layers are thus affected by the Ni layer, which produces an average ICS of −210 meV.

This average ICS of −210 meV for W(111) is quite close to our measured ICS of −230±15 meV for a ps 1×1 Ni layer on W(110). The closeness of these two shifts is not unexpected. First, the average nearest-neighbor and next-nearest-neighbor (NNN) coordination numbers of atoms in the first three W(111) surface layers are 6 and 4, respectively. These coordination numbers are identical to the NN and NNN coordination numbers of the first W(110) layer. Thus the average values of $c_Z^{(S)}$ and $c_V^{(S)}$ for the first three layers of the W(111) surface should be close to the $c_Z^{(S)}$ and $c_V^{(S)}$ values for W(110). Indeed, this is reflected in the fact that the W(111) average SCS and the W(110) SCS are so similar, −337 meV and −320 meV, respectively. Second, both the physical monolayer on W(111) and the 1×1 ps layer on W(110) correspond to 1 Ni adatom per affected surface W atom, so that the average value of $c_M^{(I)}$ for W(111) should be similar to $c_M^{(1\times1)}$ for W(110). Hence the Ni-induced shifts should be quite close for these two cases, as is observed.

Ni-layer induced core level shifts measured by Over-

bury and coworkers on W(100) are also summarized in Table 1. For 1 ps ML they observe an ICS of −120 meV. With increasing coverage this ICS smoothly decreases to −170 meV at 2 ps ML, and then remains approximately constant for higher Ni coverages. These results cannot be satisfactorily interpreted in terms of the partial-shift model developed above: the adhesion shifts on this surface are simply too large compared to the (110) and (111) surfaces. Quite surprising is the observation that W atoms under 1 layer of Ni have the same core-level binding energy as W atoms under 1 layer of W, which is clearly not observed for either of the other two low-index surfaces. It seems likely that the differences may have to do with the propensity of the (100) surface to reconstruct, even in the absence of an overlayer [91]. Again, *ab initio* calculation might shed some light on the shifts on this surface.

5. Summary

In summary, we have measured the shifts in W $4f_{7/2}$ core-level binding energies upon growth of the Ni/W(110) bimetallic interface. We have identified shifts associated with both the 1×1 pseudomorphic and 7×1 commensurate overlayers. Surprisingly, only one shift is observed for the 7×1 phase, even though not all W atoms are equivalently coordinated by Ni atoms. We suggest that this is due to the metallic nature of the bonding between the surface W and overlayer Ni atoms. It would be interesting to see if this result is a general trend in bimetallic systems.

We have further discussed the shifts in terms of the partial-shift model of Nilsson et al. [63]. The large difference in the adhesion core-level shift between the two phases indicates a substantial structural contribution to the binding-energy shifts, which may arise from the (bcc vs fcc) structural difference between the two Ni layers, a W recon-struction induced by the 7×1 Ni layer, or a combination of both effects.

Lastly, this work substantially improves upon an earlier core-level study of this same system, providing more accurate values for the core-level shifts. The shift for the 1×1 Ni/W(110) interface is consistent with the average shift induced by a physical monolayer of Ni on W(111), but is at odds with results from Ni/W(100). This discrepancy is likely due to the tendency of the W(100) surface to reconstruct.

Acknowledgments

This work was supported, in part, by the U.S. Department of Energy, Office of Basic Energy Sciences. Sandia National Laboratories is a multi-program laboratory op-erated by Sandia Corporation, a Lockheed-Martin Company, for the U. S. Department of Energy under Contract No. DE-AC04-94AL85000.

References

[1] J. Kolaczkiewicz and E. Bauer, Surf. Sci. 144 (1984) 495.

[2] J. Kolaczkiewicz and E. Bauer, Surf. Sci. 160 (1985) 1.

[3] J. Kolaczkiewicz and E. Bauer, Surf. Sci. 175 (1986) 508.

[4] P. J. Berlowitz and D. W. Goodman, Surf. Sci. 187 (1987) 463.

[5] C. Koziol, G. Lillenkamp, and E. Bauer, Appl. Phys. Lett. 51 (1987) 901.

[6] X. Mingde and R. J. Smith, J. Vac. Sci. Technol. A 9 (1990) 1828.

[7] E. Bauer, Journal of Physics: Condensed Matter 11 (1999) 9356.

[8] K.-P. Kämper, W. Schmitt, G. Güntherodt, and H. Kuhlenbeck, Phys. Rev. B 38 (1988) 9451.

[9] K.-P. Kämper, W. Schmitt, D. A. Wesner, and G. Güntherodt, Appl. Phys. A 49 (1989) 573.

[10] C. Koziol, G. Lilienkamp, and E. Bauer, Phys. Rev. B 41 (1990) 3364.

[11] R. A. Campbell, J. A. Rodriguez, and D. W. Goodman, Surf. Sci. 240 (1990) 71.

[12] N. D. Shinn, B. Kim, A. B. Andrews, J. L. Erskine, K. J. Kim, and T.-H. Kang, Material Research Society Symposium Proceedings 307 (1993) 167.

[13] P. M. Stoop, Interface Science 1 (1993) 243.

[14] J. H. van der Merwe, E. Bauer, D. L. Tönsing, and P. M. Stoop, Phys. Rev. B 49 (1994) 2127.

[15] J. K. Burdett and C. Sevov, J. Chem. Phys. 101 (1994) 840.

[16] T. C. Leung, C. L. Kao, W. S. Su, Y. J. Feng, and C. T. Chan, Phys. Rev. B 68 (2003) 195408.

[17] D. Sander, A. Enders, C. Schmidthals, D. Reuter, and J. Kirschner, Surf. Sci. 402-404 (1998) 351.

[18] D. Sander, C. Schmidthals, A. Enders, and J. Kirschner, Phys. Rev. B 57 (1998) 1406.

[19] C. Schmidthals, A. Enders, D. Sander, and J. Kirschner, Surf. Sci. 402-404 (1998) 636.

[20] C. Schmidthals, D. Sander, A. Enders, and J. Kirschner, Surf. Sci. 417 (1998) 361.

[21] H. L. Meyerheim, D. Sander, R. Popescu, J. Kirschner, O. Robach, S. Ferrer, and P. Steadman, Phys. Rev. B 67 (2003) 155422.

[22] N. A. Khan and J. G. Chen, J. Vac. Sci. Technol. A 21 (2003) 1302.

[23] N. A. Khan and J. G. Chen, J. Phys. Chem. B 107 (2003) 4334.

[24] C. M. Greenlief, P. J. Berlowitz, and D. W. Goodman, J. Phys. Chem. 91 (1987) 6669.

[25] P. Maciejewski, W. Wurth, S. Kostlmeier, G. Pacchioni, and N. Rosch, Surf. Sci. 330 (1995) 156.

[26] T. T. Magkoev, M. Song, T. Magome, and Y. Murata, Technical Physics 49 (2004) 1617.

[27] N. A. Khan and J. C. Chen, Journal of Molecular Catalysis: Chemical 208 (2004) 225.

[28] M. Farle, A. Berghaus, Y. Li, and K. Baberschke, Phys. Rev. B 42 (1990) 4873.

[29] L. Li, M. Farle, and K. Baberschke, Phys. Rev. B 41 (1990) 9596.

[30] T. Li, K. Baberschke, and M. Rarle, J. Appl. Phys. 69 (1991) 4992.

[31] Y. Li and K. Baberschke, Phys. Rev. Lett. 68 (1992) 1208.

[32] M. Farle, B. Mirwald-Schulz, A. N. Anisimov, W. Platow, and K. Baberschke, Phys. Rev. B 55 (1997) 3708.

[33] U. Bovensiepen, C. Rüdt, P. Poulopoulos, and K. Baberschke, J. Magn. Magn. Mater. 231 (2001) 65.

[34] H.-S. Rhie, H. A. Dürr, and W. Eberhardt, Phys. Rev. Lett. 90 (2003) 247201.

[35] H.-S. Rhie, H. A. Dürr, and W. Eberhardt, Appl. Phys. A 82 (2006) 9.

[36] C. S. Arnold, H. L. Johnston, and D. Venus, Phys. Rev. B 56 (1997) 8169.

[37] D. Sander, A. Enders, C. Schmidthals, J. Kirschner, H. L. Johnston, C. S. Arnold, and D. Venus, J. Appl. Phys. 81 (1997) 4702.

[38] C. S. Arnold and D. Venus, IEEE Transactions on Magnetics 34 (1998) 1039.

[39] D. Venus, C. S. Arnold, and M. Dunlavy, Phys. Rev. B 60 (1999) 9607.

[40] H. Höche and H.-J. Elmers, J. Magn. Magn. Mater. 191 (1999) 313.

[41] M. J. Dunlavy and D. Venus, Phys. Rev. B 62 (2000) 5786.

[42] We define 1 ps ML as an adsorbed density equal to the density of first-layer W atoms (1.42×10^{15} cm^{-2}) and a cp ML as an adsorbed density equal to the density of the 7×1 Ni phase (1.82×10^{15} cm^{-2}).

[43] C. Guillot, G. Tréglia, J. Lecante, D. Spanjaard, M. C. Desjonquères, d. Chauveau, Y. Jugnet, and T. M. Duc, J. Phys. C: Solid State Phys. 16 (1983) 1555.

[44] D. M. Riffe, G. K. Wertheim, and P. H. Citrin, Phys. Rev. Lett. 65 (1990) 219.

[45] G. Tréglia, M. C. Desjonquères, D. Spanjaard, Y. Lassailly, C. Guillot, Y. Jugnet, T. M. Duc, and J. Lecante, J. Phys. C: Solid State Phys. 14 (1981) 3463.

[46] C. H. F. Peden and N. D. Shinn, Surf. Sci. 312 (1994) 151.

[47] D. M. Riffe and G. K. Wertheim, Surf. Sci. 399 (1998) 248.

[48] R. X. Ynzunza*, et al.*, Surf. Sci. 459 (2000) 69.

[49] N. D. Shinn, C. H. F. Peden, K. L. Tsang, and P. J. Berlowitz, Physica Scripta 41 (1990) 607.

[50] D. M. Riffe, G. K. Wertheim, and P. H. Citrin, Phys. Rev. Lett. 64 (1990) 571.

[51] N. T. Barrett, B. Villette, A. Senhaji, C. Guillot, R. Belkhou, G. Tréglia, and B. Legrand, Surf. Sci. 286 (1993) 150.

[52] G. K. Wertheim, D. M. Riffe, and P. H. Citrin, Phys. Rev. B 49 (1994) 4834.

[53] A. B. Andrews, D. M. Riffe, and G. K. Wertheim, Phys. Rev. B 49 (1994) 8396.

[54] B. Kim, N. D. Shinn, and J. L. Erskine, Journal of the Korean Physical Society 30 (1997) 625.

[55] E. D. Tober, R. X. Ynzunza, F. J. Palomares, Z. Wang, Z. Hussain, M. A. Van Hove, and C. S. Fadley, Phys. Rev. Lett. 79 (1997) 2085.

[56] T.-W. Pi, I.-H. Hong, and C.-P. Cheng, Phys. Rev. B 58 (1998) 4149.

[57] N. P. Tucker, R. I. R. Blyth, R. G. White, M. H. Lee, C. Searle, and S. D. Barrett, J. Phys.: Condens. Matter 10 (1998)

[58] A. J. Jaworowski and A. Sandell, Surf. Sci. 477 (2001) 141.

[59] C. Gu, C. G. Olson, and D. W. Lynch, Phys. Rev. B 48 (1993) 12178.

[60] R. I. R. Blyth, C. Searle, N. P. Tucker, and S. D. Barrett, Phys. Rev. B 70 (2004) 045402.

[61] I.-H. Hong, C.-P. Cheng, and T.-W. Pi, Surf. Sci. 601 (2007) 1726.

[62] I.-H. Hong, C.-P. Cheng, and T.-W. Pi, Phys. Rev. B 75 (2007) 165412.

[63] A. Nilsson, B. Eriksson, N. Mårtensson, J. N. Andersen, and J. Onsgaard, Phys. Rev. B 38 (1988) 10357.

[64] R. G. Musket, W. McLean, C. A. Colmenares, D. M. Makowiecki, and W. J. Siekhaus, Applications of Surface Science 10 (1982) 143.

[65] T. M. Duc, C. Guillot, Y. Lassailly, J. Lecante, Y. Jugnet, and J. C. Vedrine, Phys. Rev. Lett. 43 (1979) 789.

[66] D. M. Riffe, G. K. Wertheim, and P. H. Citrin, Phys. Rev. Lett. 63 (1989) 1976.

[67] S. H. Overbury, P. F. Lyman, D. R. Mullins, and N. D. Shinn, Surf. Sci. 339 (1995) 68.

[68] H.-S. Tao, C. H. Nien, T. E. Madey, J. E. Rowe, and G. K. Wertheim, Surf. Sci. 357/358 (1996) 55.

[69] H.-S. Tao, J. E. Rowe, and T. E. Madey, Surf. Sci. 407 (1998) L640.

[70] J. J. Kolodziej, T. E. Madey, J. W. Keister, and J. E. Rowe, Phys. Rev. B 62 (2000) 5150

[71] J. J. Kolodziej, T. E. Madey, J. W. Keister, and J. E. Rowe, Phys. Rev. B 65 (2002) 075413.

[72] M. J. Gladys, G. Jackson, J. E. Rowe, and T. E. Madey, Surf. Sci. 544 (2003) 193.

[73] S. Doniach and M. Šunjic, J. Phys. C: Solid State Phys. 34 (1970) 285.

[74] P. F. Lyman and D. R. Mullins, Phys. Rev. B 51 (1995) 13623.

[75] The interfacial core-level shift is defined as the difference in binding energy between a Ni influenced core level and the binding energy of bulk W atoms.

[76] C. J. Powell and A. Jablonski, Surface and Interface Analysis 29 (2000) 108.

[77] N. Mårtensson, A. Stenborg, O. Björneholm, A. Nilsson, and J. N. Andersen, Phys. Rev. Lett. 60 (1988) 1731.

[78] B. Johansson and N. Mårtensson, Phys. Rev. B 21 (1980) 4427.

[79] B. Johansson and N. Mårtensson, Helvetica Physica Acta 56 (1983) 405.

[80] D. Spanjaard, C. Guillot, M. C. Desjonquères, G. Tréglia, and J. Lecante, Surface Science Reports 5 (1985) 1.

[81] M. Said, M. C. Desjonquères, and D. Spanjaard, Surf. Sci. 287/288 (1993) 780.

[82] E. Lundgren, M. Qvarford, R. Nyholm, and J. N. Andersen, Vacuum 46 (1995) 1159.

[83] L. Vitos, A. V. Ruban, H. L. Skriver, and J. Kollár, Surf. Sci. 411 (1998) 186.

[84] A. V. Ruban, H. L. Skriver, and J. K. Nørskov, Phys. Rev. B 59 (1999) 15990.

[85] F. R. de Boer, R. Boom, W. C. M. Mattens, A. R. Miedema, and A. K. Niessen, Cohesion in Metals: Transition Metal Alloys (North-Holland, New York, 1988).

[86] A. V. Ruban, H. L. Skriver, and J. K. Nørskov, Phys. Rev. Lett. 80 (1998) 1240.

[87] M. Aldén, H. L. Skriver, and B. Johansson, Phys. Rev. Lett. 71 (1993) 2449.

[88] C. Kittel, Solid State Physics (Wiley, New York, 2005).

[89] K. G. Purcell, J. Jupille, G. P. Derby, and D. A. King, Phys. Rev. B 36 (1987) 1288.

[90] G. K. Wertheim and P. H. Citrin, Phys. Rev. B 38 (1988) 7820.

[91] I. K. Robinson, A. A. MacDowell, M. S. Altman, P. J. Estrup, K. Evans-Lutterodt, J. D. Brock, and R. J. Birgeneau, Phys. Rev. Lett. 62 (1989) 1294